Improved Accuracy for Interferometric Radar Images Using Polarimetric Radar and Laser Altimetry Data

K. Clint Slatton, Melba M. Crawford, and Brian L. Evans

The University of Texas at Austin
E-mail: slatton@csr.utexas.edu, Ph: +1.512.471.5509, Fax: +1.512.471.3570

Center for Space Research
The University of Texas at Austin

Introduction

- Terrain topography can be determined over large areas using interferometric radar (INSAR)
  - Synthetic aperture radar (SAR) produces complex-valued images
  - Cross-correlating two images yields a phase ϕ used to solve for terrain heights z_S [1]
- Vegetation introduces error into height measurements
  - Scattering from both ground and vegetation leads to ambiguity ($z_g \le z_S \le z_v$)

$$\phi = \underbrace{\frac{2\pi}{\lambda}\left(\rho_{S2} - \rho_{S1}\right)}_{geometry} \approx \underbrace{\frac{-2\pi}{\lambda} B\sin\left(\theta_S - \alpha\right)}_{system\ parameters} \rightarrow \begin{aligned} z_S &= h_S - \rho_{S1}\cos\theta_S \\ y_S &= \rho_{S1}\sin\theta_S \end{aligned}$$

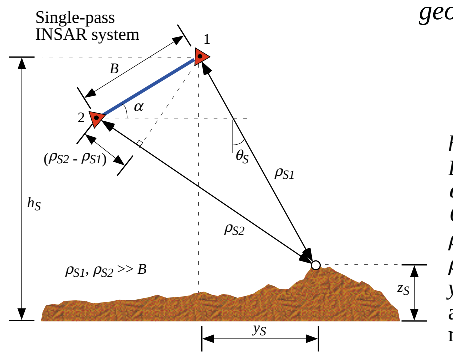

h_S = altitude of antenna 1
B = baseline distance
α = baseline angle
θ_S = incidence angle
ρ_{S1} = path length from antenna 1
ρ_{S2} = path length from antenna 2
y_S and z_S = target coordinates
azimuth direction is out of the plane
range direction is to the right

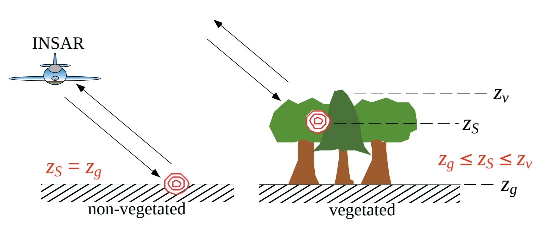

Method 1: Data Fusion

- Two-step approach
  - Reduce measurement noise in z_S image with adaptive minimum mean squared error filter → z_{Sf}
  - Use SAR and laser altimeter (LIDAR) images to correct z_{Sf} for vegetation errors → z_{Sc}
- Classify SAR magnitude images to locate pixels containing vegetation [2]
- Determine class-dependent height corrections using LIDAR data
  - LIDAR has limited coverage, but high vertical resolution

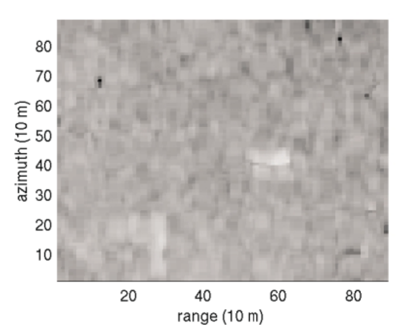

INSAR height image (λ = 5.7 cm): z_S

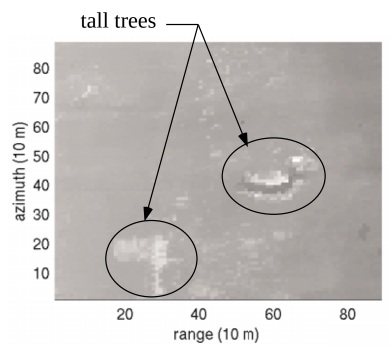

LIDAR height image (λ = 1047 nm): z_L

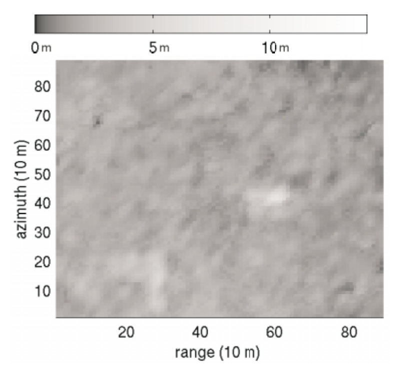

Corrected INSAR height image: z_{Sc}

Method 1 Results

- Achieve 6% reduction in global mean squared error (MSE) relative to filtering alone
- Disadvantages
  - Requires LIDAR and multiple-polarization SAR data
  - Still must overcome inherent ambiguity of INSAR height measurement over vegetation

Class-dependent height offsets added to z_{Sf}

Barren	-0.23 m
Medium	0.03 m
Trees	0.20 m

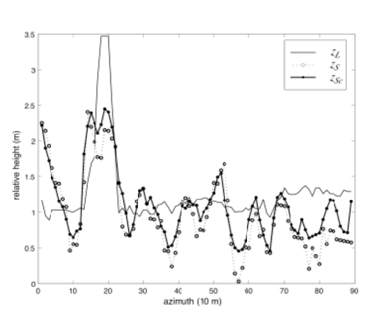

Transects from column 23 of test images

Square root of MSE (SMSE) relative to LIDAR after noise reduction z_{Sf} and after noise reduction plus vegetation correction z_{Sc}. ΔMSE_{Global} is percent reduction in global MSE from unfiltered z_S.

z_{Sf}		z_{Sc}	
$SMSE_{Barren}$	0.72 m	$SMSE_{Barren}$	0.69 m
$SMSE_{Medium}$	0.50 m	$SMSE_{Medium}$	0.50 m
$SMSE_{Trees}$	0.63 m	$SMSE_{Trees}$	0.59 m
$SMSE_{Global}$	0.60 m	$SMSE_{Global}$	0.57 m
ΔMSE_{Global}	13%	ΔMSE_{Global}	19%

Method 2: Solve an Inverse Problem

- Relate INSAR measurement to ground and vegetation heights
  - Use electromagnetic scattering model $\boldsymbol{A}$ to relate observations $\boldsymbol{b}$ to terrain parameters $\boldsymbol{x}$ [3]
  - Observation vector $\boldsymbol{b}$ is 4 x 1 vector of magnitude and phase for two INSAR images

$$\boldsymbol{b} = \boldsymbol{A}(\boldsymbol{x}) \qquad \boldsymbol{x} = \begin{bmatrix} \Delta z_v \\ z_g \\ \tau \end{bmatrix}$$

Δz_v = vegetation height above ground
z_g = ground elevation
τ = vegetation extinction coefficient

- Transform inverse problem into constrained nonlinear optimization problem
  - Inequality constraints bound feasible region $\boldsymbol{X}$

$$\begin{gathered} \min \quad p(\boldsymbol{x}) \\ \text{subject to } g(\boldsymbol{x}) \le \boldsymbol{0} \\ p : \mathrm{R}^3 \rightarrow \mathrm{R}^1 \end{gathered} \qquad \begin{gathered} \boldsymbol{x} \in \boldsymbol{X} \subseteq \mathrm{R}^3 \\ p(\boldsymbol{x}) = \left\| \boldsymbol{A}(\boldsymbol{x}) - \boldsymbol{b} \right\|_2 \end{gathered}$$

$$0 < \theta_S < \pi/2$$

$$\boldsymbol{X} = \left\{ \begin{bmatrix} \Delta z_v \\ z_g \\ \tau \end{bmatrix} : \begin{bmatrix} 0\text{ m} & < \Delta z_v < & 12\text{ m} \\ 0\text{ m} & < z_g < & \min(z_g) + 20\text{ m} \\ 0\,\text{dB/m} & < \tau < & 0.6\text{ dB/m} \end{bmatrix} \right\}$$

- Objective function and constraints are twice differentiable and convex on feasible region
- Model as sequential quadratic programming problem [4]

Method 2 Results

- Using simulated terrain data
  - Include measurement noise and random variations in free parameters $\{\Delta z_v, z_g, \tau\}$
- Magnitude is scaled relative to phase to improve convergence
- No phase wrapping in feasible region
- Robust to choice of initial guess

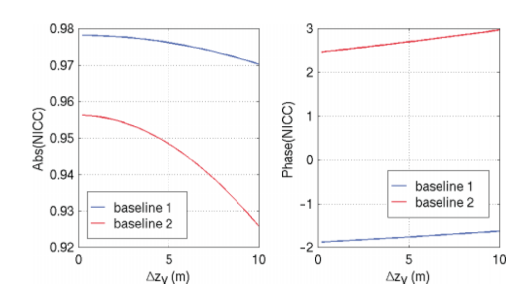

Variation of $\boldsymbol{b}$ with vegetation height. NICC is normalized interferometric cross correlation

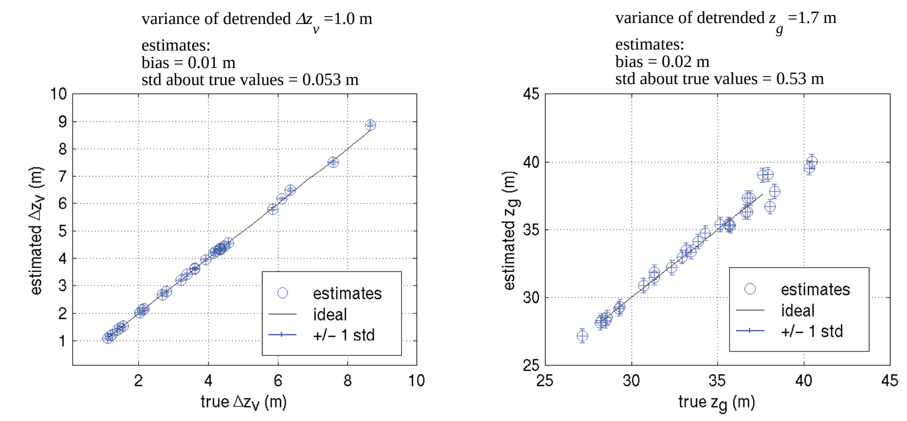

Estimates of ground and vegetation heights versus true values

Conclusions

- Two methods developed to correct errors in INSAR images due to vegetation
  - Data fusion approach employed adaptive linear filtering and combining of LIDAR and SAR data
  - Inversion approach employed scattering models and nonlinear optimization
- Data fusion method
  - Takes advantage of complementary measurement types
  - Achieves moderate improvement in z_{Sc}
- Inversion method
  - Directly solves for desired parameters and does not require additional data types
  - Shows promise, but must be tested on real data

Future Work

- Combine methods 1 and 2
  - Solve inverse problem to separate Δz_v and z_g random processes
  - Apply adaptive linear filtering and data fusion techniques to Δz_v and z_g images
- Use scattering model that includes surface scattering
- Consider contextual information during optimization
- Re-train SAR imagery classifier to better isolate tall vegetation

Acknowledgments

This work was supported by the National Aeronautics and Space Administration, under the Topography and Surface Change Program (Grant NAG5-2954) and the Graduate Student Research Fellowship Program (Grant NGT-50239).

References

[1] F. Li and R. M. Goldstein, "Studies of multi-baseline spaceborne interferometric synthetic aperture radars," *IEEE Trans. Geosci. Remote Sensing*, vol. 28, no. 5, pp. 88-97, 1990.

[2] M. M. Crawford, S. Kumar, M. R. Ricard, J. C. Gibeaut, and A. Neuenschwander, "Fusion of Air-borne Polarimetric and Interferometric SAR For Classification of Coastal Environments," *IEEE Trans. Geosci. Remote Sensing*, vol. 37, no. 3, pp. 1306-1315, 1999.

[3] R. N. Treuhaft and P. R. Siqueira, "Vertical structure of vegetated land surfaces from interferometric and polarimetric radar," *Radio Science*, vol. 35, no. 1, pp. 141-177, 1999.

[4] M. S. Bazaraa, H. D. Sherali, and C. M. Shetty, *Nonlinear Programming: Theory and Algorithms*, John Wiley and Sons, Inc., 2nd ed., New York, NY, 1993.